Available online at www.sciencedirect.com
SCIENCE DIRECT®
Journal of Sound and Vibration 281 (2005) 375–398
JOURNAL OF SOUND AND VIBRATION
www.elsevier.com/locate/jsvi

On the non-linear vibrations of an inextensible rotating arm with setting angle and flexible hub

M.N. Hamdan[a], A.H. El-Sinawi[b,*]

[a]*Department of Mechanical Engineering, University of Jordan, Amman, Jordan*
[b]*Department of Mechanical Engineering, King Fahd University of Petroleum and Minerals, Dhahran 31261, Saudi Arabia*

Received 29 October 2002; accepted 11 December 2003

Abstract

This work is concerned with the development of a dynamic model for a slender flexible arm undergoing relatively large planar flexural deformations, and clamped with a setting angle to a compliant rotating hub. The model is derived assuming an inextensible Euler–Bernoulli beam, but takes into account the axial inertia and nonlinear curvature. Two coordinate transformations were used to obtain the inertial position vector of a typical material point along the beam span. The inextensibility constraint is used to relate the axial and transverse displacements as well as velocities of the material point in the beam body coordinate system. The displacement and velocity vectors obtained are used in the system kinetic energy and exact curvature to eliminate dependence of the system Lagrangian on the beam axial deflection and velocity. The assumed mode method is used to discretize the system Lagrangian and to derive, directly, the nonlinear equivalent temporal solutions to the problem. The resulting dynamic model is a set of four strongly coupled nonlinear ordinary differential equations, which, in the present work, is solved only numerically. Examples of the results of the numerical solutions for the effects of setting angle and defined physical parameter ratios on the system dynamic response characteristics for a sinusoidal hub torque profile are presented and discussed.

*Corresponding author. Tel.: +966-3-860-2455; fax: +966-3-860-2949.
E-mail addresses: mnader@ju.edu.jo (M.N. Hamdan), elsinawi@kfupm.edu.sa (A.H. El-Sinawi).

0022-460X/$ - see front matter © 2004 Elsevier Ltd. All rights reserved.
doi:10.1016/j.jsv.2003.06.036

1. Introduction

The characteristics of dynamic response of a rotating flexible beam element are of major concern in many important industrial applications such as the design of robotic arms, satellite antenna, and turbine blades. To meet the demands of high rotating speeds, fast response and accurate positioning modern designs use lighter weight, more flexible and axially rigid rotating beam elements. It is well known that the axial displacement due to bending deformations, known as axial shortening, and the axial inertia associated with a high rotating speed, have a significant effect on the flexural vibrations of such flexible rotating beam elements. These flexural vibrations have been the subject of many analytical and numerical investigations, e.g. Refs. [1–18]. These investigations use different mathematical models with various simplifying assumptions concerning the beam geometric nonlinearities and various ways of accounting for the effect of axial shortening due to bending; for recent reviews of relevant literature, see, for example, Refs. [15–18]. This has led to significantly different results depending on the way the shortening effect is accounted for in the formulation of equations of motion [14]. In several cases, the method of virtual work was used to account only partially for the effect of axial shortening in the formulation of either the stiffness or inertia forces. This led to unstable behaviour at high values of the rotation speed [14]. In order to obtain stable high rotation speed motions, some models accounted for the shortening effect in the formulation of both the inertia and elastic forces [14]. Again, when using the method of virtual work, this was only partially done by ignoring some of the nonlinear terms which may arise as a result of axial shortening. Note that the type (inertia and elastic) and degree of nonlinearities in the mathematical model, and thus the predicted behaviour, depend on the way the shortening effect is accounted for in the formulation of the system equations of motion. Recently, Hamdan and Al-Bedoor [16] used the in-extensibility condition, in conjunction with a straightforward multi-body dynamic approach, to account for the effects of axial shortening due to bending in the formulation of both the potential and kinetic energies of a flexible beam attached with a setting angle to a rotating rigid hub. Their model, which covers both in-plane (lead-lag) and out-of-plane (flapping) beam-bending motions, includes elastic and inertial geometric stiffening nonlinear terms as well as competing nonlinear inertia softening terms not found in other available models. They then used the assumed mode method in conjunction with Lagrangian dynamics to reduce their model to a single-degree-of-freedom (d.o.f.) nonlinear unforced oscillator. They presented an approximate analytic solution to their model, which shows that the beam-bending vibration, at any mode, remains stable as the rotation speed is increased to significantly high values. The results of their study also showed that the setting angle has a significant effect on the natural frequency corresponding to any of the modes of the beam-bending vibrations. These results also indicate that for a setting angle below a critical value, the first mode bending free vibration of the rotating beam may become unstable for low rotation speed. A systematic multi-body dynamic approach in conjunction with the inextensibilty condition to account for axial shortening due to bending has also recently been used by Al-Bedoor and Hamdan [15] to study the dynamic response characteristics of a rotating beam attached to a rigid hub with zero setting angle, and also by Al-Bedoor et al. [17] to study the effect of hub support flexibility of the rotating beam [15]. Models which accounted for the effect of setting angle of the rotating beam were reported by several other investigations. For example, Yokoyama [6] and Mulmule et al. [9] used the finite element method to study flexural free vibrations of a rotating

beam with a setting angle, where the axial shortening due to bending was accounted for in the form of added potential energy term. In both of these models, the effect of geometric stiffening due to the combined axial shortening and centrifugal forces disappears as a result of the approach used when the setting angle becomes 90°.

A model for a rotating beam element which accounts for the combined effects of setting angle and hub flexibility is to the authors' best knowledge not readily available in the open literature. To this end, the aim of the present work is to develop a mathematical model and to present simulation results for the dynamic behaviour of a rotating blade modelled as a flexible slender beam attached with a setting angle to a rigid rotating hub. The hub is assumed to be supported by a compliant base and subjected to a prescribed torque profile. A multi-body dynamic approach, which employs two transformation matrices, is used to obtain the inertial displacement vector for a typical material point along the span of the rotating blade from a body coordinate system. The first of these two transformations takes care of the setting angle, which is a constant parameter that may vary in the range of 0–90°. The second transformation is used to account for the system rigid body rotation. The condition of inextensibility is used to relate the axial and lateral components of the material point deflection. The inertial velocity vector obtained, which accounts for lateral as well as axial inertia of the beam, is used to obtain the system kinetic energy, which includes the base 2 d.o.f. translational motion and rigid body rotation of the hub–arm system. The nonlinear curvature is used to construct the beam elastic potential energy. Lagrangian dynamics in conjunction with the assumed single-mode method is used to develop an equivalent third-order temporal model consisting of four nonlinear coupled ordinary differential equations. The four independent variables in the model obtained are: the horizontal and vertical position of the hub–arm assembly, the rigid body rotation of the hub, and the transverse deflection of the beam in the modal domain. As a result of using the inextensibility condition, the model includes elastic and inertial stiffening and inertial softening nonlinearities not found in other rotating beam models available. Due to its mathematical complexity, this model is in the present work only solved numerically for selected values of system parameters. The results of numerical simulation are presented and are used to investigate the effect, for the first and third bending modes, of system parameters on the dynamic behaviour of the rotating beam.

2. The dynamic model

2.1. System description and assumptions

The arm–hub system under consideration is shown schematically in Fig. 1. X, Y, Z denote the set of inertial rectangular Cartesian coordinate axes fixed in space. x, y, z is the set of orthogonal axes rotating with the hub with origin o at the root of the beam (i.e., on the hub surface) and with the x-axis oriented along the beam neutral axis in the undeformed configuration. x', y', z' are the beam principal axes in the undeformed configuration with common origin o with xyz axes. The beam mid-plane $y'z'$ is inclined to the plane of rotation yz at an angle Ψ called the setting angle. The hub is assumed to be a rigid disc with radius R_H, mass m_H, rotating with angular velocity $\dot{\theta}$ and subjected to a torque T about an axis through its centre parallel to the inertial Z-axis. The base of the hub is assumed to be flexible with linear stiffnesses K_X and K_Y in the horizontal and

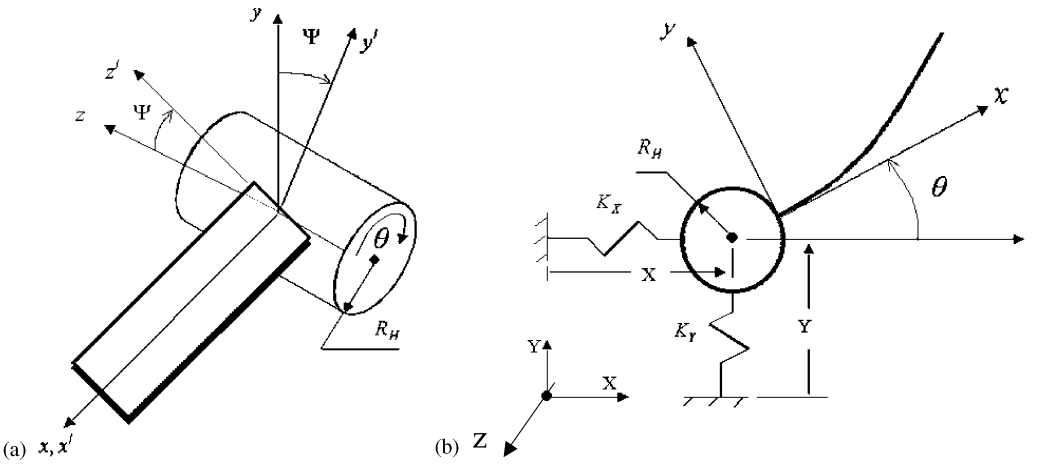

Fig. 1. Arm–hub schematic diagram: (a) setting angle, (b) hub base flexibility.

vertical directions, respectively. The beam is assumed to be initially straight along the x'-axis, clamped at the base, having uniform cross-sectional area A, flexural rigidity EI, constant length l and mass per unit volume ρ. The beam thickness is assumed to be small compared to its length so that the effects of shear deformation and rotary inertia can be ignored. The beam deflection is assumed to be confined to the $x'y'$-plane (that is, only planar flexural beam vibrations are allowed). This vibration is purely in the xy-plane (lead-lag) when $\Psi = 0^\circ$ and is purely in the xz-plane (flapping) when $\Psi = 90^\circ$. In the following sub-sections, the governing equations of motion are formulated via a combined Lagrange-assumed mode method wherein the inextensibility condition and its time derivative are used to account for axial shortening due to bending and to eliminate the dependence of the system Lagrangian on axial displacement and axial velocity.

2.2. System kinetic and potential energies

Using the coordinate systems shown in Figs. 1 and 2, the inertial X, Y, Z components of the global displacement vector $\vec{R}_P$ of the beam cross-sectional area centroid P at an arbitrary point s along the span of the beam after deformation are given by

$$\begin{Bmatrix} R_{PX} \\ R_{PY} \\ R_{PZ} \end{Bmatrix} = \begin{Bmatrix} R_{OX} \\ R_{OY} \\ 0 \end{Bmatrix} + \begin{Bmatrix} R_H \cos\theta \\ R_H \sin\theta \\ 0 \end{Bmatrix} + [A(\theta)][A(\Psi)] \begin{Bmatrix} s-u \\ v \\ 0 \end{Bmatrix}, \tag{1}$$

where $R_{OX} = X$, $R_{OY} = Y$ are, respectively, the X and Y inertial components of the position vector $\vec{R}_O$ of the hub centre o, R_H is the hub radius, θ is the rigid body rotation of the beam–hub system about the inertial Z-axis, Ψ is the setting angle, and $[A(\theta)]$ is the rotational transformation matrix from the xyz rotating coordinate system to the fixed XYZ coordinate

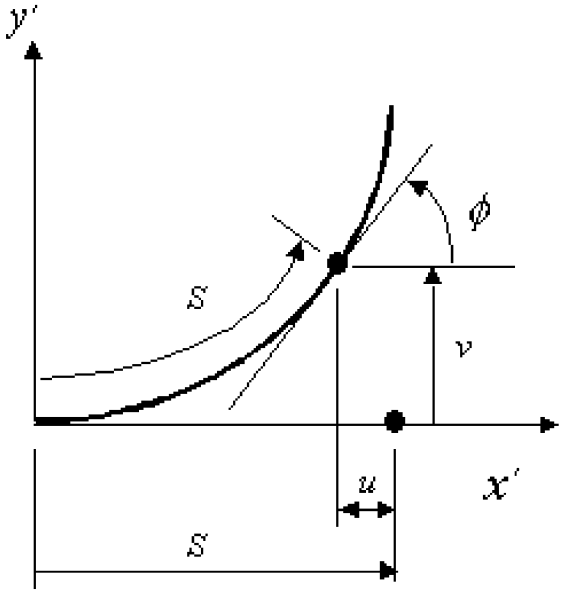

Fig. 2. Deflected configuration of the beam.

system given by

$$[A(\theta)] = \begin{bmatrix} \cos\theta & -\sin\theta & 0 \\ \sin\theta & \cos\theta & 0 \\ 0 & 0 & 0 \end{bmatrix}, \tag{2}$$

$[A(\Psi)]$ is the setting angle transformation matrix from the $x'y'z'$ beam-rotating coordinate system to the xyz hub-rotating coordinate system defined by

$$[A(\Psi)] = \begin{bmatrix} 1 & 0 & 0 \\ 0 & \cos\Psi & -\sin\Psi \\ 0 & \sin\Psi & \cos\Psi \end{bmatrix}, \tag{3}$$

where $u = u(s,t)$ is the axial displacement (shortening due to bending) of the deformed beam at the material point P along the rotating x'-axis, and $v = v(s,t)$ is the transverse deflection of P along the rotating y'-axis due to the beam-bending deformation.

The components of the inertial velocity vector $\bar{R}_P$ of the material point P are obtained by differentiating Eq. (1), which yields

$$\begin{bmatrix} \dot{R}_{PX} \\ \dot{R}_{PY} \\ \dot{R}_{PZ} \end{bmatrix} = \begin{bmatrix} \dot{X} - \dot{\theta} R_H \sin\theta \\ \dot{Y} + \dot{\theta} R_H \cos\theta \\ 0 \end{bmatrix} + \dot{\theta} \left[\frac{\mathrm{d}A(\theta)}{\mathrm{d}\theta}\right] [A(\Psi)] \begin{Bmatrix} s-u \\ v \\ 0 \end{Bmatrix} + [A(\theta)][A(\Psi)] \begin{Bmatrix} -\dot{u} \\ \dot{v} \\ 0 \end{Bmatrix}, \tag{4}$$

where $\dot{\theta}$ is the absolute angular velocity of the beam–hub system with respect to the inertial Z-axis, and

$$\left[\frac{\mathrm{d}A(\theta)}{\mathrm{d}\theta}\right] = \begin{bmatrix} -\sin\theta & -\cos\theta & 0 \\ \cos\theta & -\sin\theta & 0 \\ 0 & 0 & 0 \end{bmatrix}. \tag{5}$$

Substituting Eqs. (2), (3) and (5) into Eq. (4) and carrying out matrix multiplications in the resulting equations gives the following expressions for the inertial velocity vector $\vec{R}_P$ of the beam material point P:

$$\dot{\vec{R}}_P = (\dot{X} - \alpha_1 \sin\theta - \alpha_2 \cos\theta)\vec{I} + (\dot{Y} - \alpha_2 \sin\theta + \alpha_1 \cos\theta)\vec{J} + (\dot{v} \sin\Psi)\vec{K}, \tag{6}$$

$$\alpha_1 = \dot{\theta}(\mathrm{R}_H + (s-u)) + \dot{v}\cos\Psi, \quad \alpha_2 = \dot{\theta}v\cos\Psi + \dot{u}, \tag{6a, b}$$

where $\vec{I}, \vec{J}$, and $\vec{K}$ are, respectively, unit vectors along the X, Y and Z inertial axes. The kinetic energy KE_b of the uniform, inextensible rotating beam is given by

$$\mathrm{KE}_b = \frac{\rho A}{2}\int_0^l \dot{\vec{R}}_P \cdot \dot{\vec{R}}_P \,\mathrm{d}s, \tag{7}$$

where $\dot{\vec{R}}_P$ is given by Eq. (6). The total kinetic energy KE of the hub–beam system is obtained by adding to Eq. (6) the kinetic energy of the hub KE_H, which is assumed to be a uniform disc of radius R_H, mass m_H, rotating at angular velocity $\dot{\theta}$ about the inertial Z-axis and translating against two linear springs in the vertical and horizontal directions as shown in Fig. 1. Accordingly, the hub kinetic energy KE_H is given by

$$\mathrm{KE}_H = \tfrac{1}{2}m_H\dot{X}^2 + \tfrac{1}{2}m_H\dot{Y}^2 + \tfrac{1}{4}m_H R_H^2\dot{\theta}^2. \tag{8}$$

The total kinetic energy KE of beam–hub system is expressed as

$$\mathrm{KE} = \mathrm{KE}_b + \mathrm{KE}_H, \tag{9}$$

where KE_b and KE_H are, respectively, given by Eqs. (7) and (8). Note that the system total kinetic energy KE in Eq. (9) is dependent on the beam displacement and velocity variables $u, v, \dot{u}$ and $\dot{v}$ in addition to the hub centre o horizontal and vertical velocities, respectively, $\dot{X}$ and $\dot{Y}$, as well as on the hub rotation speed $\dot{\theta}$. The dependence of KE on the axial displacement u and axial velocity $\dot{u}$ can be eliminated by assuming the beam to be undergoing an inextensible planar bending motion. This requires that the beam axial shortening u corresponding the lateral deflection v of this inextensible planar bending motion is given by [19]

$$\lambda u(\xi, t) = \xi - \int_0^\xi \cos\phi(\eta, t)\,\mathrm{d}\eta, \tag{10}$$

where $\lambda = 1/l$, $\xi = s/l$ is a dimensionless beam arc length and ϕ (see Fig. 2), is the slope of the beam centre line at arc position ξ. Noting that $\sin\phi = \mathrm{d}v/\mathrm{d}s = \lambda v' < 1$, where a prime denotes a derivative with respect to the dimensionless arc length ξ, $\cos\phi = \sqrt{1-\sin^2\phi}$, expanding the term $[\{1-(\lambda v')^2]^{1/2}$ into power series, and retaining terms up to fourth order, the axial shortening

expression in Eq. (10) simplifies to

$$u = \tfrac{1}{2}\int_0^{\xi} [\lambda v'^2 + \tfrac{1}{2}\lambda^3 v'^4]\,\mathrm{d}\eta. \tag{11}$$

Differentiating Eq. (11) with respect to time yields the following expression for the beam axial velocity $\dot{u}$ in terms of its transverse bending deflection:

$$\dot{u} = \frac{1}{2}\frac{\mathrm{d}}{\mathrm{d}t}\left[\int_0^{\xi} [\lambda v'^2 + \lambda^3 v'^4]\,\mathrm{d}\eta\right]. \tag{12}$$

Eqs. (11) and (12) will be used to eliminate the dependence of the system kinetic energy, and thus the system Lagrangian on the beam axial displacement u and axial velocity $\dot{u}$. Next, in order to formulate the system Lagrangian, the system potential energy PE is constructed . For the present beam–hub system, the potential energy PE, assuming the system to rotate in a horizontal plane (that is, ignoring gravity), is made up of the beam elastic bending energy and the elastic potential energy PE_H due to hub translation against the linear springs at the base. The potential energy PE_b of the beam due to the assumed inextensible planar bending motion is given by

$$\mathrm{PE}_b = \frac{\mathrm{EI}}{2\lambda}\int_0^1 K^2(\xi, t)\,\mathrm{d}\xi \tag{13}$$

where EI is the beam principal flexural rigidity about the z'-axis, $\lambda = 1/l$ and $\xi = s/l$ as defined above, and K is the centre line curvature at a point ξ. Following the analysis presented in Ref. [19], note, using Fig. 2, that

$$K(\xi, t) = \lambda\phi', \tag{14}$$

$$\sin\,\phi = \lambda v', \tag{15}$$

where, as before, ϕ is the beam centreline slope at a position ξ, and a prime denotes a derivative with respect to the dimensionless arc length ξ. Again, as before, differentiating Eq. (15), and using the relation $\cos\,\phi = \sqrt{1 - \sin^2\phi} = \sqrt{1 - (\lambda v')^2}$ gives

$$\phi' = \lambda v''[1 - (\lambda v')^2]^{-1/2}. \tag{16}$$

Upon substituting Eq. (16) into Eq. (14), noting that $\lambda v' < 1$, expanding the bracketed term $[1 - (\lambda v')^2]^{-1/2}$ in the resulting equation into power series, retaining terms up to fourth order and substituting the result into Eq. (14), yields the following expression for the beam-bending potential energy $\mathrm{PE_b}$:

$$\mathrm{PE}_b = \frac{(\mathrm{EI}\lambda^3)}{2}\int_0^1 [v''^2 + (\lambda v' v'')^2]\,\mathrm{d}\xi, \tag{17}$$

which is independent of the beam axial displacement u or any of its derivatives. Adding the elastic potential energy PE_H due to system translation against the base linear springs to Eq. (17) yields

the system total potential energy expression PE:

$$\mathrm{PE} = \tfrac{1}{2}K_X X^2 + \tfrac{1}{2}K_Y Y^2 + \frac{(\mathrm{EI}\lambda^3)}{2}\int_0^1 [v''^2 + (\lambda v' v'')^2]\,\mathrm{d}\xi. \tag{18}$$

2.3. System Lagrangian

The Lagrangian L of the present rotating hub–beam system is given by

$$L = \mathrm{KE} - \mathrm{PE}, \tag{19}$$

where KE and PE are defined by Eqs. (9) and (18), respectively. Substituting these equations into Eq. (19), and using the relations in Eqs. (6)–(8), (11) and (12), noting that the independent variable $\dot{\theta}$ is independent of the dimensionless spatial variable ξ, and introducing appropriate dimensionless system parameters and variables, yields the following expression for the system Lagrangian L:

$$\begin{aligned}
L = {} & \frac{m_b l^2}{2}\left[(\dot{\bar{X}}^2 + \dot{\bar{Y}}^2)(1+\mu) + \dot{\theta}^2\left(\tfrac{1}{3} + C + C^2(1+\mu/2)\right) + \dot{\theta}\left[(1+2C)(\dot{\bar{Y}}\cos\theta - \dot{\bar{X}}\sin\theta\right]\right] \\
& + \frac{m_b l^2}{2}\int_0^1 \left\{ \left[\frac{1}{4}\frac{\mathrm{d}}{\mathrm{d}t}\left(\int_0^\xi \left[w'^2 + \tfrac{1}{4}w'^4\right]\mathrm{d}\eta\right)\right]^2 + \dot{w}^2 + \dot{\theta}^2\left[\tfrac{1}{4}\int_0^\xi \left(w'^2 + \tfrac{1}{4}w'^4\right)\mathrm{d}\eta\right]^2 + w^2\dot{\theta}^2\cos^2\Psi \right. \\
& + \left[\dot{\theta}(\dot{\bar{X}}\sin\theta - \dot{\bar{Y}}\cos\theta - \dot{w}\cos\Psi) + \dot{\theta}^2(C-\xi)\right]\int_0^\xi \left(w'^2 + \tfrac{1}{4}w'^4\right)\mathrm{d}\eta \\
& + (w\dot{\theta}\cos\Psi - \dot{\bar{X}}\cos\theta - \dot{\bar{Y}}\sin\theta)\frac{\mathrm{d}}{\mathrm{d}t}\left[\int_0^\xi \left(w'^2 + \tfrac{1}{4}w'^4\right)\mathrm{d}\eta\right] + 2\dot{w}\cos\Psi[\dot{\bar{Y}}\cos\theta \\
& - \dot{\bar{X}}\sin\theta + \dot{\theta}(C+\xi)] - 2\dot{\theta}\cos\Psi(\dot{\bar{X}}\cos\theta + \dot{\bar{Y}}\sin\theta)w - \beta^2\left[S_1\bar{X}^2 + S_2\bar{Y}^2\right] \\
& \left. + \int_0^1 \left[w''^2 + (w'w'')^2\right]\right\}\mathrm{d}\xi,
\end{aligned} \tag{20}$$

where $C = R_H/l$, and $\mu = m_H/m_b$ are, respectively, dimensionless hub radius-to-beam length ratio and hub mass-to-beam mass ratio, $S_1 = K_X l^3/\mathrm{EI}$ and $S_2 = K_Y l^3/\mathrm{EI}$ are dimensionless flexibility parameters, $\beta = (\mathrm{EI}/m_b l^3)^{1/2}$ is a frequency parameter, $\bar{X} = X/l$ and $\bar{Y} = Y/l$ are hub centre o dimensionless displacements along the inertial X and Y axes, respectively, and $w = v/l$ is the dimensionless beam flexural deflection along the body y'-axis.

Note that the system Lagrangian L in Eq. (20) is a function of the beam transverse dimensionless deflection w, which is a continuous function of the spatial variable ξ and time t. In the present work, in order to avoid the elaborate task of deriving the field partial differential equations of motion, this continuous Lagrangian is discretized using the assumed mode method. Assuming the beam vibration to be dominated by a single mode gives

$$w = q(t)\Phi(\xi), \tag{21}$$

where $\Phi(\xi)$ is a normalized, self-similar mode shape deflection of the beam and $q(t)$ is the corresponding time modulation modal coordinate. In the present work, the assumed mode shape function $\Phi(\xi)$ is taken to be that of the associated non-rotating linear cantilevered beam

given by

$$\Phi(\xi) = \left(\frac{1}{r}\right)[\cosh p\xi - \cos p\xi - \gamma(\sinh p\xi - \sin p\xi)], \tag{22}$$

where $r = \left|\Phi(\xi)\right|_{\xi=1}$ is a scaling factor, and $p^4 = m_b\omega^2 l^3/(\mathrm{EI})$ (ω is the assumed mode natural frequency of the non-rotating linear cantilever beam) is a frequency parameter of the assumed linear mode obtained by solving the transcendental frequency equation:

$$\cos p \cosh p + 1 = 0 \tag{23}$$

and γ is a weighting constant of the assumed mode given by

$$\gamma = \frac{(\sinh p - \sin p)}{(\cosh p + \cos p)}. \tag{24}$$

Substituting for Eq. (21) into Eq. (20), leads to the following discrete expression of the system Lagrangian L:

$$\begin{aligned} L = \frac{m_b l^2}{2}\Big\{ & (1+\mu)(\dot{\bar{X}}^2 + \dot{\bar{Y}}^2) + C_0\dot{\theta}^2 + \beta_1\dot{q}^2 - \beta^2(S_1\bar{X}^2 + S_2\bar{Y}^2 + \beta_2 q^2) \\ & - (1+2C)\dot{\bar{X}}\theta\sin\theta + (1+2C)\dot{\bar{Y}}\dot{\theta}\cos\theta - 2\beta_3\dot{\theta}q\cos\Psi(\dot{\bar{X}}\cos\theta + \dot{\bar{Y}}\sin\theta) \\ & + \beta_4 q^2\dot{\theta}(\dot{\bar{X}}\sin\theta - \dot{\bar{Y}}\cos\theta) + (C\beta_4 - \beta_6 + \beta_1\cos^2\Psi)q^2\dot{\theta}^2 \\ & + \beta_5\dot{\theta}q^2\dot{q}\cos\Psi + 2\cos\Psi(\beta_7 - C\beta_3)\dot{q}\dot{\theta} + 2\beta_3\dot{q}\cos\Psi(\dot{\bar{Y}}\cos\theta - \dot{\bar{X}}\sin\theta) \\ & -\beta^2\beta_9 q^4 - 2\beta_4 q\dot{q}(\dot{\bar{X}}\cos\theta + \dot{\bar{Y}}\sin\theta) + \beta_8 q^2\dot{q}^2 * (1+\mu)(\dot{\bar{X}}^2 + \dot{\bar{Y}}^2) * \Big\}, \end{aligned} \tag{25}$$

where $C_0 = C + \frac{1}{3} + C^2(1+\mu/2)$ and

$$\begin{aligned} & \beta_1 = \int_0^1 \Phi^2\,\mathrm{d}\xi, \quad \beta_2 = \int_0^1 \Phi''^2\,\mathrm{d}\xi, \quad \beta_3 = \int_0^1 \Phi\,\mathrm{d}\xi, \quad \beta_4 = \int_0^1 \left(\int_0^\xi \Phi'^2\,\mathrm{d}\eta\right)\mathrm{d}\xi, \\ & \beta_5 = \int_0^1 \Phi\left(\int_0^1 \Phi'^2\,\mathrm{d}\eta\right)\mathrm{d}\xi, \quad \beta_6 = \int_0^1 \xi\left(\int_0^\xi \Phi'^2\,\mathrm{d}\eta\right)\mathrm{d}\xi, \quad \beta_7 = \int_0^1 \xi\left(\int_0^\xi \Phi\,\mathrm{d}\eta\right)\mathrm{d}\xi, \\ & \beta_8 = \int_0^1 \left(\int_0^\xi \Phi'^2\,\mathrm{d}n\right)^2\mathrm{d}\xi, \quad \beta_9 = \int_0^1 \Phi'^2\Phi''^2\,\mathrm{d}\xi. \end{aligned} \tag{26}$$

In addition to the above system Lagrangian, the virtual work δW done by the externally applied hub torque T is given by

$$\delta W = T\delta\theta. \tag{27}$$

2.4. Equations of motion

Applying Euler–Lagrange equation

$$\frac{\mathrm{d}}{\mathrm{d}t}\left(\frac{\partial L}{\partial \dot{g}_i}\right) - \frac{\partial L}{\partial g_i} = 0, \quad i = 1,\ldots,4, \tag{28}$$

where $g_1 = \bar{X}, g_2 = \bar{Y}, g_3 = q$ and $g_4 = \theta$ are the Lagrangian independent generalized coordinates, and using Eq. (27) to account for the effect of the externally applied torque T, leads to the following set of four, coupled, of order three nonlinearities, ordinary differential equations of motion:

$$(1+\mu)\ddot{\bar{X}} + \beta^2 S_1 \bar{X} + \left[-\frac{(1+2C)}{2}\cos\theta + \beta_3(\cos\Psi\sin\theta)q + \frac{\beta_4}{2}q^2\cos\theta\right]\dot{\theta}^2 - \left[\frac{(1+2C)}{2}\sin\theta - \beta_3(\cos\Psi\cos\theta)q - \left(\frac{\beta_4}{2}\sin\theta\right)q^2\right]\ddot{\theta} - (2\beta_3\cos\Psi\cos\theta)\dot{q}\dot{\theta} + 2\beta_4\sin\theta)q\dot{q}\dot{\theta} - \left[\beta_3\cos\Psi\sin\theta + \beta_4(\cos\theta)q\right]\ddot{q} - (\beta_4\cos\theta)\dot{q}^2 = 0, \tag{29}$$

$$(1+\mu)\ddot{\bar{Y}} + \beta^2 S_2 \bar{Y} - \left[\frac{(1+2C)}{2}\sin\theta + (\beta_3\cos\Psi\cos\theta)q - \frac{\beta_4}{2}(\sin\theta)q^2\right]\dot{\theta}^2 + \left[\frac{(1+2C)}{2}\cos\theta - \beta_3(\cos\Psi\sin\theta)q - \frac{\beta_4}{2}(\cos\theta)q^2\right]\ddot{\theta} - 2\beta_4(\cos\theta)q\dot{q}\dot{\theta} - 2\beta_3(\cos\Psi\sin\theta)\dot{q}\dot{\theta} + [\beta_3\cos\Psi\cos\theta - \beta_4(\sin\theta)q]\ddot{q} - \beta_4(\sin\theta)\dot{q}^2 = 0, \tag{30}$$

$$(\beta_1 + \beta_8 q^2)\ddot{q} - \left[\beta_3\cos\Psi\sin\theta + (\beta_4\cos\theta)q\right]\ddot{\bar{X}} + [\beta_3\cos\Psi\cos\theta - (\beta_4\sin\theta)q]\ddot{\bar{Y}} + \left[(\beta_7 - C\beta_3)\cos\Psi + \tfrac{1}{2}(\beta_5\cos\Psi)q^2\right]\ddot{\theta} + [\beta^2\beta_2 - (C\beta_4 - \beta_6 + \beta_1\cos^2\Psi)\dot{\theta}^2]q + \beta_8 q\dot{q}^2 + 2\beta^2\beta_9 q^3 = 0, \tag{31}$$

$$\left[C_0 + (C\beta_4 - \beta_6 + \beta_1\cos^2\Psi)q^2\right]\ddot{\theta} + \cos\Psi\left[\beta_7 - C\beta_3 + \tfrac{1}{2}\beta_5 q^2\right]\ddot{q} + (\beta_5\cos\Psi)q\dot{q}^2 - \left[\frac{(1+2C)}{2}\sin\theta + \beta_3(\cos\Psi\cos\theta)q - \frac{\beta_4}{2}(\sin\theta)q^2\right]\ddot{\bar{X}} + \left[\frac{(1+2C)}{2}\cos\theta - \beta_3(\cos\Psi\cos\theta)q - \frac{\beta_4}{2}(\cos\theta)q^2\right]\ddot{\bar{Y}} + 2(C\beta_4 - \beta_6 + \beta_1\cos^2\Psi)q\dot{q}\dot{\theta} = \frac{T}{m_b l^2}. \tag{32}$$

The above four coupled, of order three nonlinearities, ordinary differential Eqs. (29)–(32) model the planar nonlinear vibrations of the hub–beam system, shown in Figs. 1 and 2, rotating under the action of the externally applied torque T to the hub. The d.o.f.'s in this model are the rigid body rotation θ, the hub base dimensionless displacements $\bar{X}$ and $\bar{Y}$ in the horizontal and vertical directions, respectively, and the dimensionless modal beam tip lateral flexural deflection q. The above model, as a result of assuming in-extensional beam-bending deflection includes nonlinear inertial softening as well as nonlinear inertial stiffening terms. For example, as a result of using the in-extensibility conditions given by Eqs. (11) and (12), the above model includes the inertial nonlinear softening $q^2\ddot{q}$ and hardening (i.e. competing) $q\dot{q}^2$ terms due to the kinetic energy of the beam local axial motion as well as other coupling inertial nonlinear terms (i.e. $q^2\ddot{\theta}, q^2\ddot{\bar{X}}, q^2\ddot{\bar{Y}}$). A realistic investigation of the dynamic behaviour of the system requires approximate analytic solutions to be obtained using, i.e., the harmonic balance method, and

carrying out stability and bifurcation analysis of the approximate solution. However, due to the nature of these equations, this is a rather involved task that goes beyond the intended scope of the present work. Instead, the dynamic behaviour of the system is explored in the present work through a numerical simulation procedure, whereby Eqs. (29)–(32) are numerically integrated for selected values of system parameters and a prescribed torque T profile. Examples of the numerical simulation results obtained are presented and discussed in the next section.

3. Numerical simulation and discussion

Numerical simulation of the dynamic model in Eqs. (29)–(32) was carried out, for the first and third modes of the beam-bending vibrations, using specially developed MATLAB software. It begins with the evaluation of the coefficients in Eq. (26) assuming system physical properties, given in Table 1, which are like those of the system used in Refs. [17,18] and a selected value of the beam-setting angle Ψ. As was done in Ref. [18], the inverse dynamic procedure was used to design an open loop positioning torque, which accounts for the given rigid body inertia. Fig. 3 shows a typical sinusoidal torque profile needed to rotate the system, with a setting angle $\Psi = 0^0$ and a relatively rigid base stiffness with stiffness coefficients $S_1 = S_2 = 10^6$, an angle $\theta = 22.5^\circ$ in 5 s. The resulting time variation profiles of the hub angular position θ, hub angular velocity $\dot{\theta}$, horizontal hub displacement $\bar{X}$, vertical hub displacement $\bar{Y}$, and associated beam tip deflection q, for the first mode of the beam-bending vibrations are displayed in Figs. 4–7. Examples of the effects on the profile of beam tip deflection q correspond to the first and third modes of linear beam-bending vibration of varying the setting angle Ψ and base stiffness coefficients S_1 and S_2 are shown in Figs. 8–21. Note that, depending on the selected range of its parameters, the response of the present highly nonlinear model in Eqs. (29)–(32) is expected to exhibit complicated nonlinear behaviour (i.e. internal and combination resonance, aperiodic and quasi-periodic responses), and other nonlinear behaviours. The results in Figs. 4–21 show the effect of varying hub-base stiffness coefficients and beam-setting angle only for the system with hub–beam physical characteristics shown in Table 1. A more realistic investigation of the system response would require employing geometric and approximate analytic methods of modern nonlinear theory for a wide range of system parameters, which is beyond the scope of the present work. Based on the present ''limited'' exploratory numerical results shown in Figs. 4–21, however, the following remarks are made:

(1) For a rigid base, after the removal of the applied sinusoidal hub torque, the beam-bending deflection, hub angular velocity and hub horizontal and vertical deflections oscillate at a

Table 1
Arm-hub data

Arm length l	3 m
Arm flexural rigidity EI	756 N/m^2
Arm mass per unit length ρA	4.0125 kg/m
Hub radius R_H	0.2 m
Hub mass m_H	50 kg

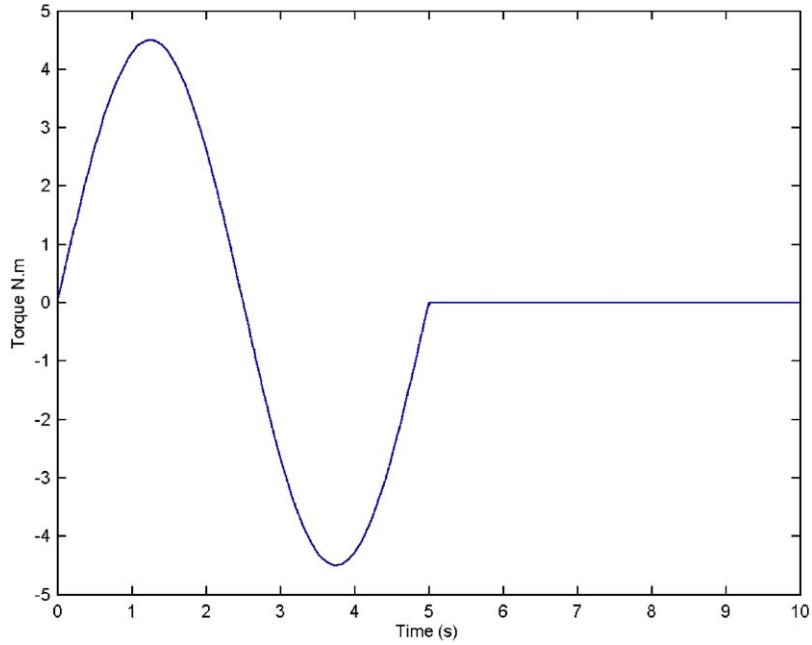

Fig. 3. Torque profile.

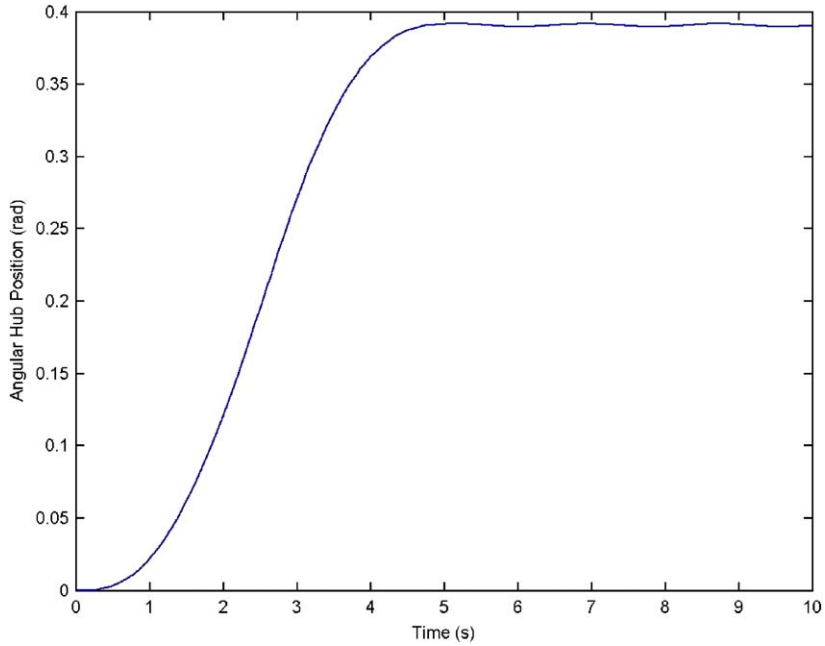

Fig. 4. Angular hub position (first mode).

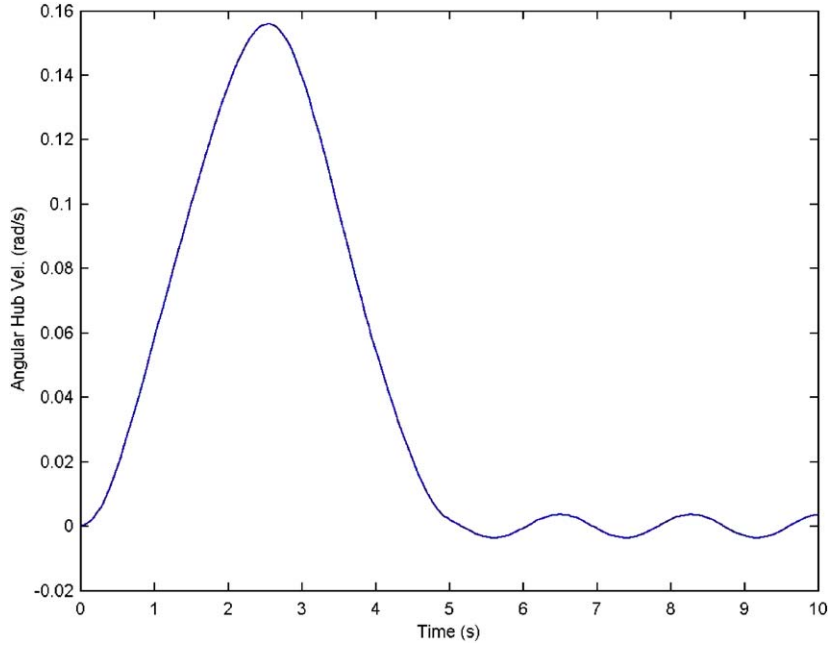

Fig. 5. Angular hub velocity (first mode).

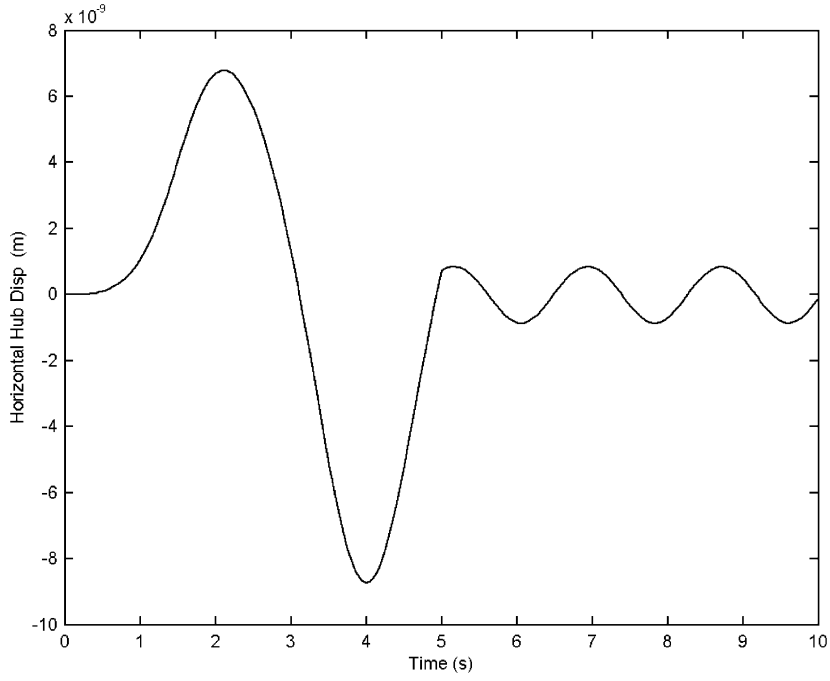

Fig. 6. Horizontal hub displacement (first mode).

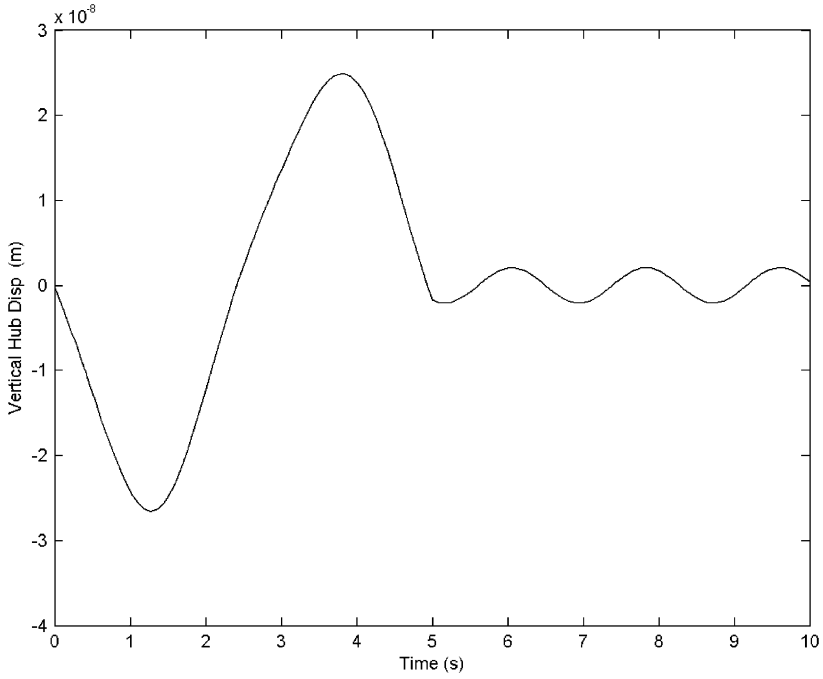

Fig. 7. Vertical hub displacement (first mode).

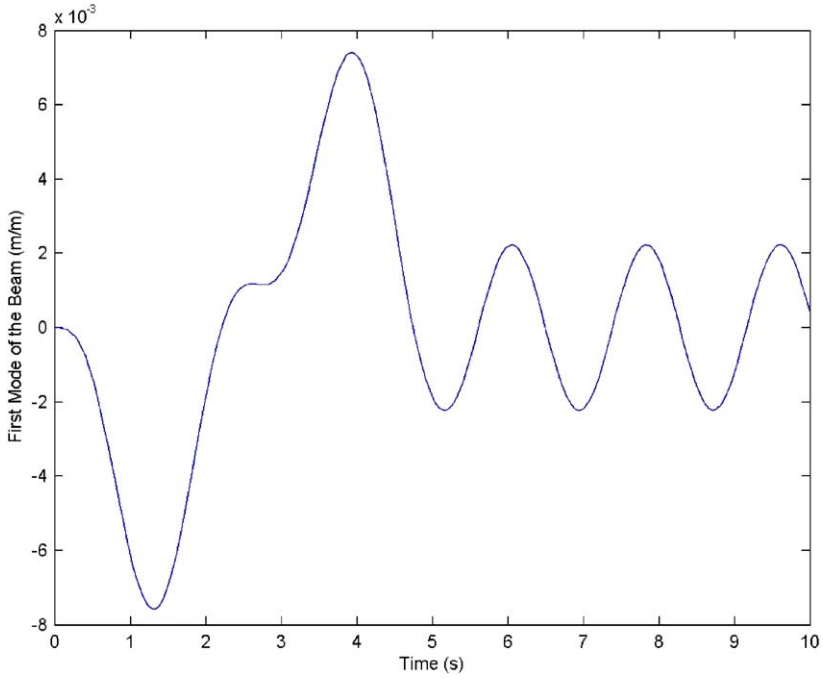

Fig. 8. Tip deflection for setting angle $\Psi = 0^\circ$ (first mode).

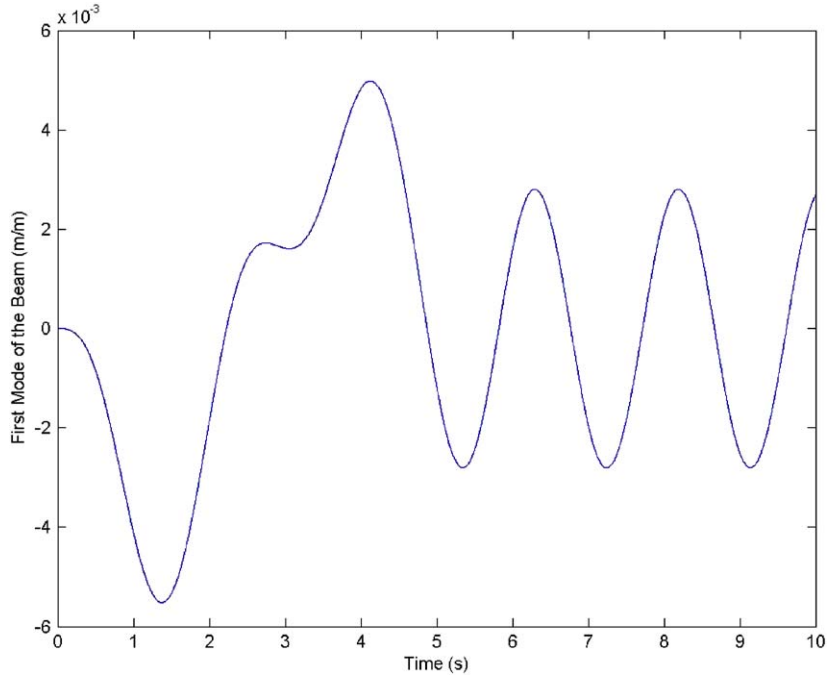

Fig. 9. Tip deflection for setting angle $\Psi = 45^\circ$ (first mode).

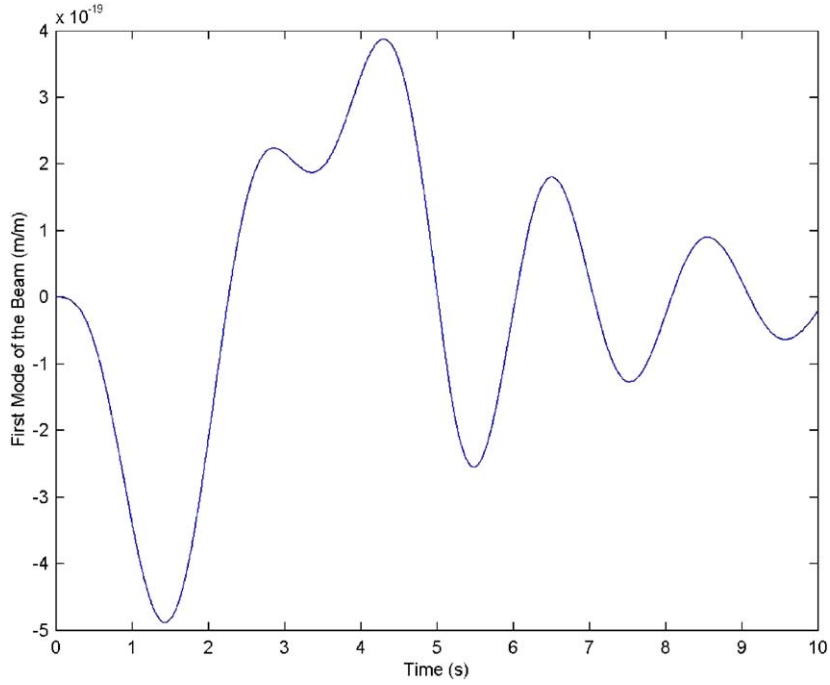

Fig. 10. Tip deflection for setting angle $\Psi = 90^\circ$ (first mode).

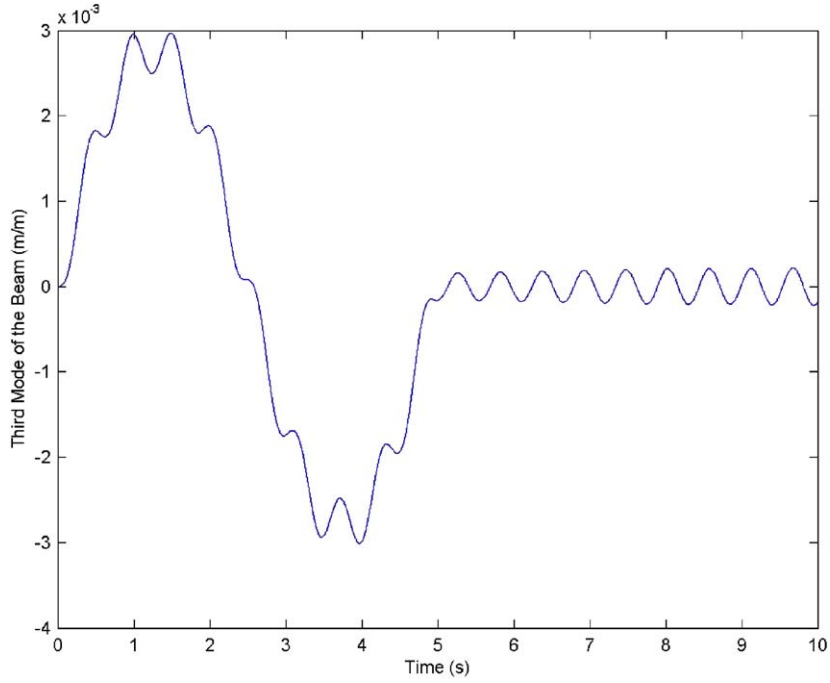

Fig. 11. Tip deflection for setting angle $\Psi = 0^\circ$ (third mode).

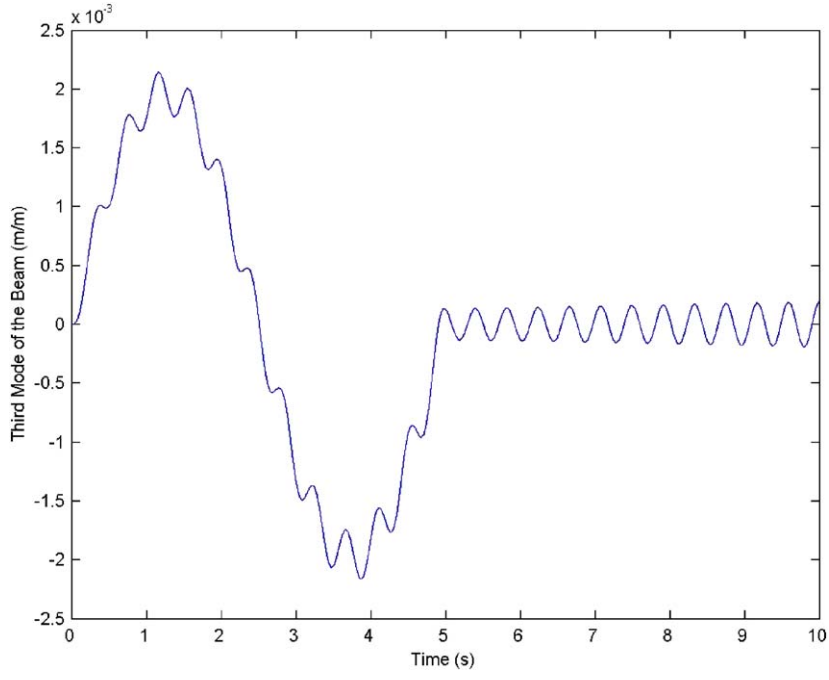

Fig. 12. Tip deflection for setting angle $\Psi = 45^\circ$ (third mode).

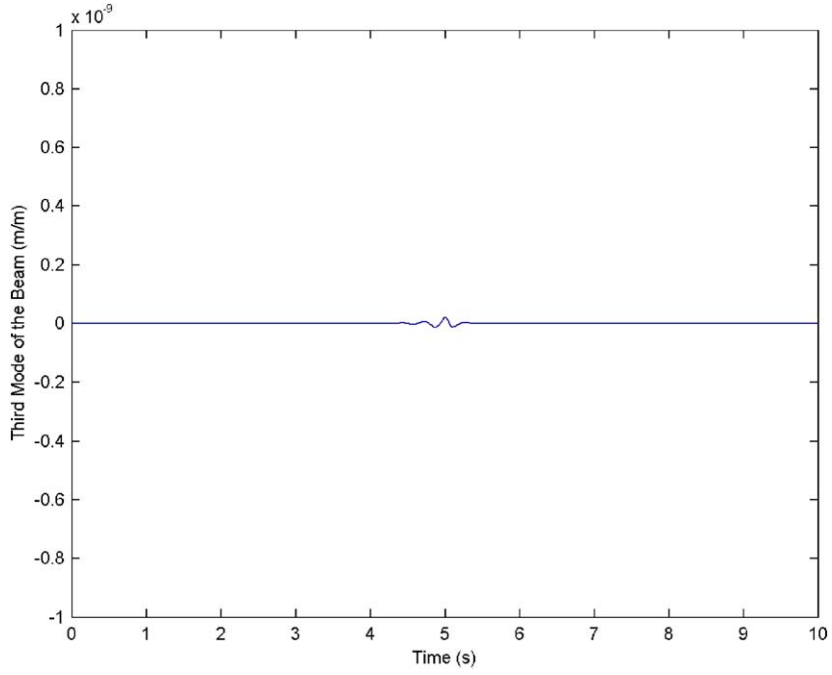

Fig. 13. Tip deflection for setting angle $\Psi = 90^\circ$ (third mode).

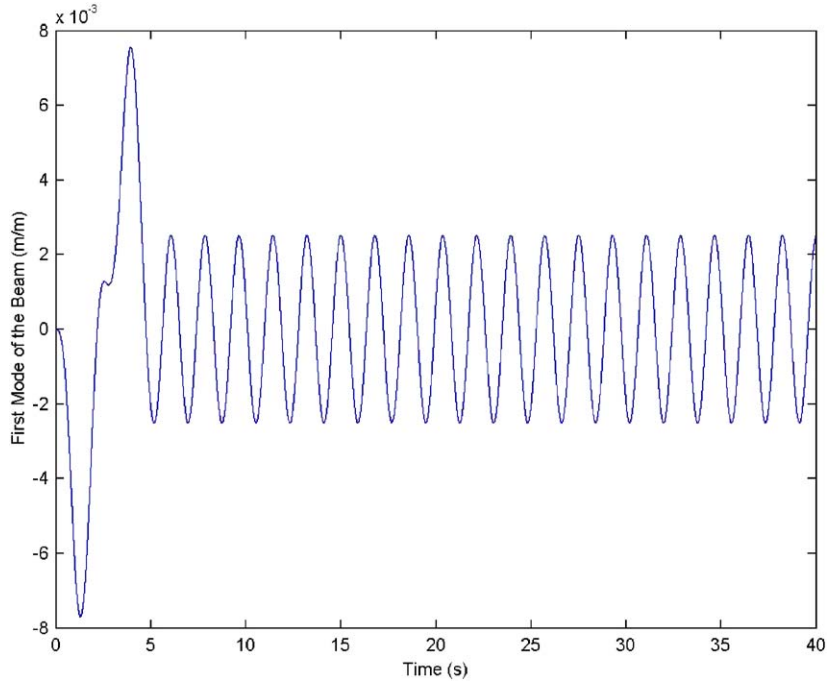

Fig. 14. Tip deflection for setting angle $\Psi = 0^\circ$ and low hub stiffness ratio (first mode).

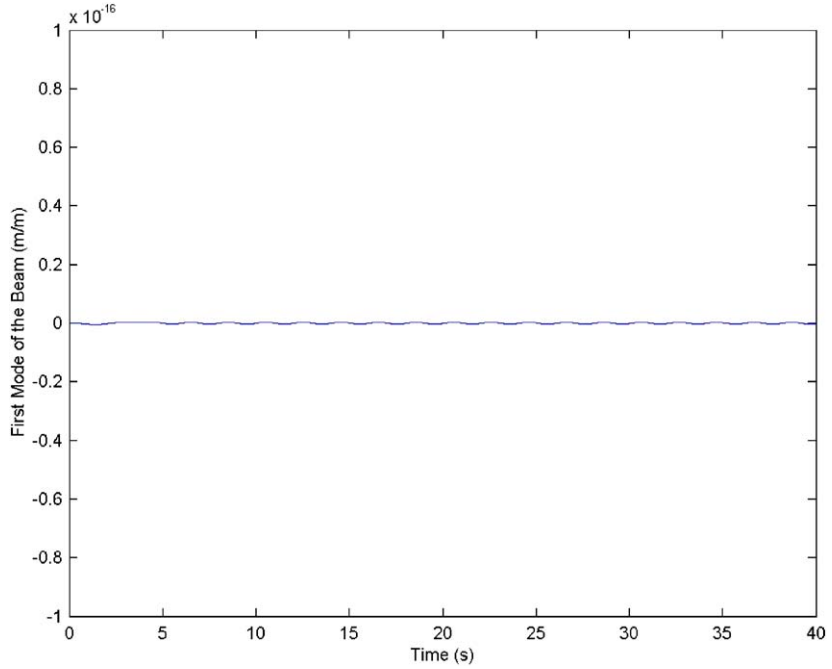

Fig. 15. Tip deflection for setting angle $\Psi = 90^\circ$ and low hub stiffness ratio (first mode).

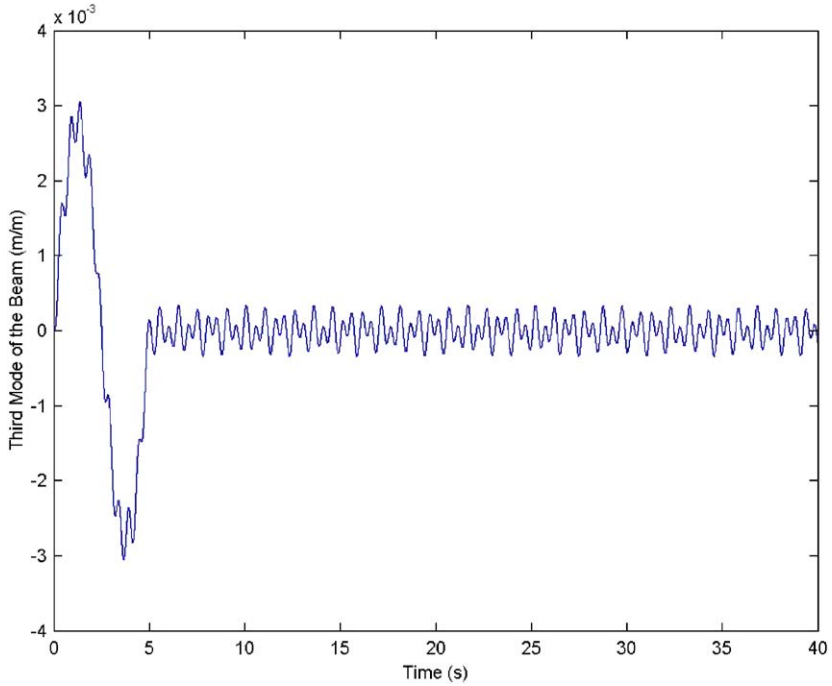

Fig. 16. Tip deflection for setting angle $\Psi = 0^\circ$ and low hub stiffness ratio (third mode).

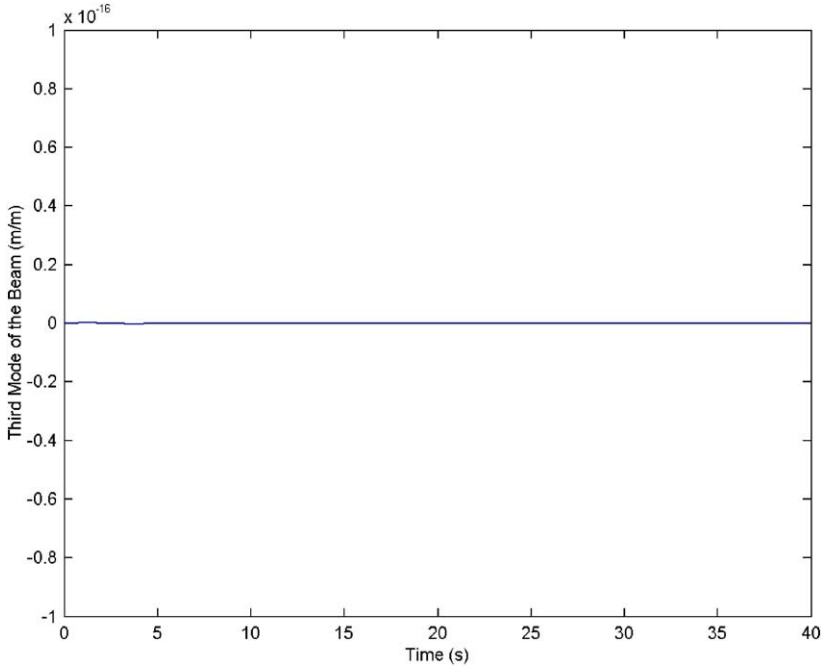

Fig. 17. Tip deflection for setting angle $\Psi = 90^\circ$ and low hub stiffness ratio (third mode).

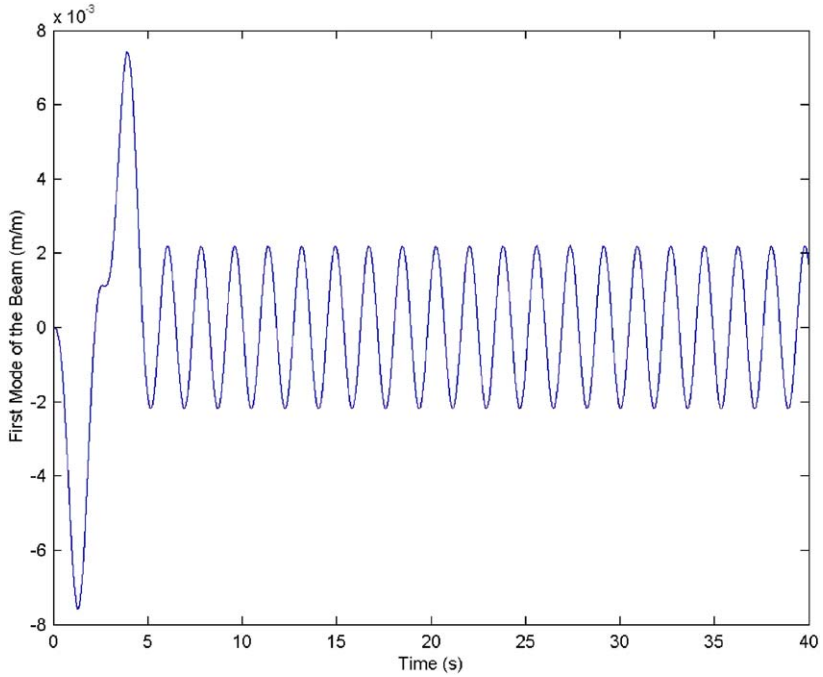

Fig. 18. Tip deflection for setting angle $\Psi = 0^\circ$, $S_1 = 100$, and $S_2 = 10^6$ (first mode).

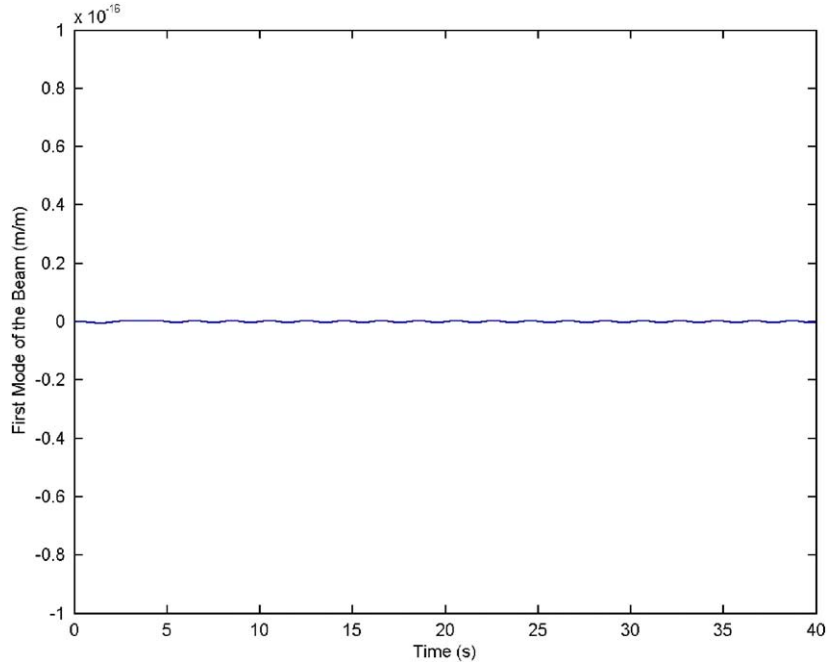

Fig. 19. Tip deflection for setting angle $\Psi = 90^\circ$, $S_1 = 100$, and $S_2 = 10^6$ (first mode).

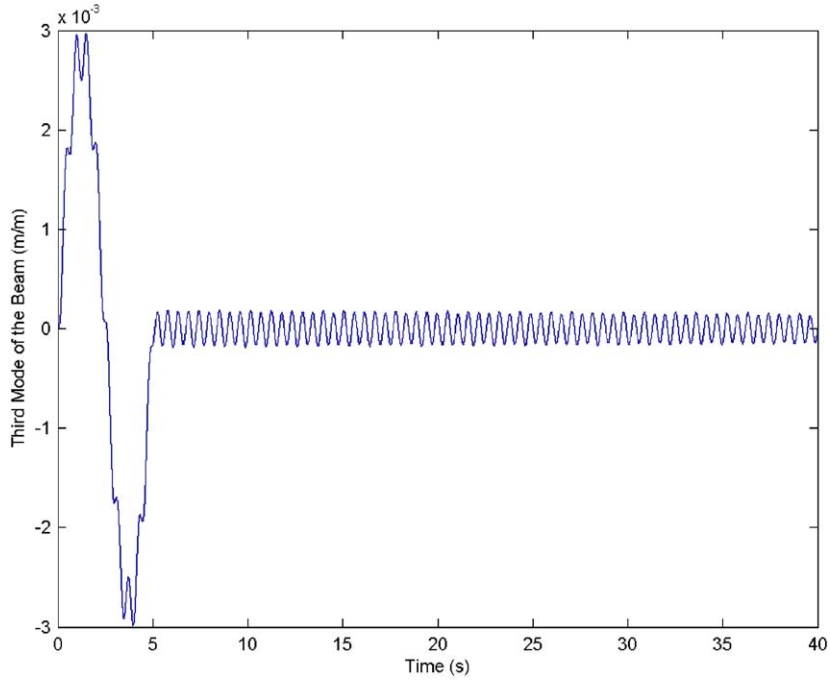

Fig. 20. Tip deflection for setting angle $\Psi = 0^\circ$, $S_1 = 100$, and $S_2 = 10^6$ (third mode).

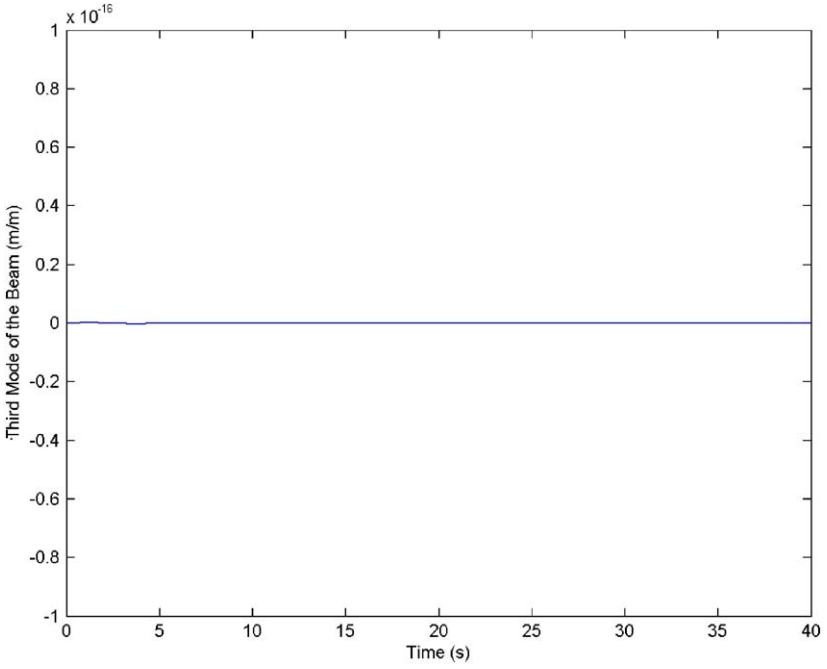

Fig. 21. Tip deflection for setting angle $\Psi = 90^\circ$, $S_1 = 100$, and $S_2 = 10^6$ (third mode).

system natural frequency, which depends on, but is far removed from, that of the assumed linear beam mode. For example, it can be seen from Figs. 5–8 that the hub angular velocity, beam tip deflection and hub horizontal and vertical deflections after 5 s (i.e., after the applied hub torque is removed) exhibit harmonic oscillations, the frequency of which is ≈ 3.1 rad/s for the first assumed mode and ≈ 9.4 rad/s for the third mode, where, for the given beam characteristics, the corresponding linear bending mode frequency is ≈ 9.133 rad/s for the first mode and ≈ 160.3 rad/s for the third mode. Note that this similarity of the hub horizontal and hub vertical displacement waveforms with that of the beam tip deflection may, in part, justify the common practice of measuring a rotating blade (beam) bending vibration using a vibration sensor attached to the base of hub.

(2) As the base stiffness is reduced to a relatively low value, the beam tip deflection for each of the assumed modes tends to exhibit, for both the in plane (setting angle $\Psi = 0^0$) and flapping ($\Psi = 90^0$) cases, nonlinear vibrations during application and after removal of the applied hub torque. The results shown in Figs. 14–17 and others not shown indicate that the amplitude for some of these nonlinear beam tip bending vibrations shows a slow and continuous build-up to larger values and eventually becomes unstable. Furthermore, the waveform of the beam tip vibration does not, in this case, seem to resemble either that of the base horizontal or the vertical displacement of the hub.

(3) Except for the relatively soft hub-base, the beam's setting angle Ψ appears to have a significant effect on the beam tip vibrations. It can be seen from Figs. 8, 10, 11, 13, 20 and 21 that as the setting angle Ψ is increased to 90° the beam tip vibration (flapping), as one expects, almost diminishes after removal of the applied torque. For an intermediate value of Ψ, i.e. for

$\Psi = 45^\circ$ the results shown in Figs. 9 and 12 indicate that the beam vibration which is partly in-plane and partly flapping may have an amplitude larger than that of the in-plane case ($\Psi = 0^\circ$).

It is worth mentioning that the system goes through a very short transient response at $t = 5+$ s. This short transient appears as a discontinuity at the instant the torque hub is removed as seen , for example, in Figs. 6, 7, 11 and 12. However, expanding this region in the relevant figures (e.g., see Fig. 22), shows a transient response rather than a discontinuity.

4. Conclusion

The nonlinear dynamic response characteristics of a rotating inextensible flexible beam clamped with a setting angle to a compliant hub rotating under the influence of an externally applied toque are numerically simulated using a consistently formulated mathematical model, which takes into account the beam axial inertia and nonlinear curvature. The developed model employs the multi-body dynamic approach to account for the system rigid body rotation and beam-setting angle by using two transformation matrices. The Lagrangian dynamics in conjunction with the assumed mode method is used to derive directly the equivalent temporal problem of four coupled, of order three nonlinearities, ordinary differential equations. As a result of assuming inextensible

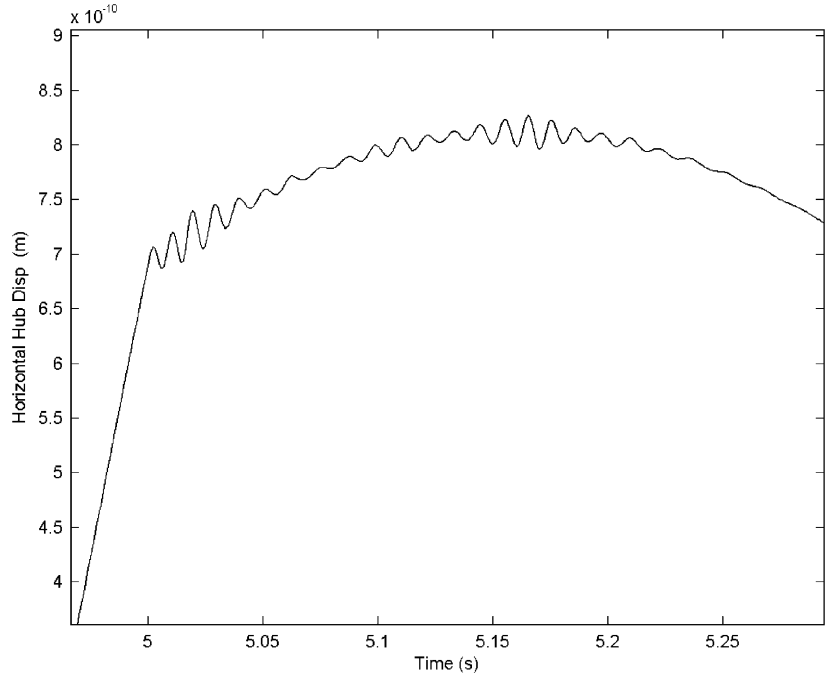

Fig. 22. Expansion of the region in the vicinity of $t = 5$ s in Fig. 6, which shows a high-frequency transient response of the hub.

beam-bending motion, the effect of axial displacement and its associated axial inertia due to bending were consistently incorporated into the system Lagrangian. This has led to nonlinear effects (i.e. softening as well as hardening), which in general are not accounted for in other dynamic models. The model was simulated numerically to explore the effects of system parameters, namely, setting angle and base stiffness, on the system dynamic behaviour as the system is driven by a prescribed torque to a given angular position. The results of this numerical simulation indicate that a soft base in combination with a low setting angle can lead to unstable beam vibrations, which makes the problem of designing a strategy for controlling the beam tip position for such a case a difficult task. Finally, it is noted that the dynamic response of the highly nonlinear system model in Eqs. (29)–(32), which depends on several parameters, may exhibit complicated nonlinear behaviours, that is aperiodic, quasi-periodic and bifurcations, as its parameters changed over their range, which can only be realistically investigated using modern geometric and approximate analytical methods of nonlinear theory along with numerical simulations.

Acknowledgments

The authors acknowledge the support of the University of Jordan and King Fahd University of Petroleum and Minerals.

References

[1] L. Shilhansil, Bending frequencies of a rotating cantilever beam, *Journal of Applied Mechanics* 25 (1958) 28–30.
[2] D. Pnuelli, Natural bending frequency comparable to rotational frequency in rotating cantilever beam, *Journal of Applied Mechanics* 39 (1972) 602–604.
[3] P.W. Likins, Mathematical modeling of spinning elastic bodies, *AIAA Journal* 9 (1973) 1251–1258.
[4] K. Kaza, R. Kvaternik, Non-linear flap-lag-axial equations of a rotating beam, *AIAA Journal* 15 (1977) 871–874.
[5] N.G. Stephens, P.J. Wang, Stretching and bending of a rotating beam, *Journal of Applied Mechanics* 53 (1986) 869–872.
[6] T. Yokoyama, Free vibration characteristics of rotating Timoshinko beams, *International Journal of Mechanical Science* 30 (1988) 743–755.
[7] T.P. Mitchell, J.C. Bruch Jr., Free vibrations of a flexible arm attached to a compliant finite hub, *Journal of Vibration, Acoustics, Stress and Reliability in Design* 110 (1988) 118–120.
[8] Y.C. Pan, R.A. Scott, A.G. Ulsoy, Dynamic modeling and simulation of flexible robots with prismatic joints, *Journal of Mechanical Design* 112 (1990) 307–314.
[9] S. Mulmule, G. Singh, G. Venkateswara Rao, Flexural vibration of rotating tapered Timoshinko beams, *Journal of Sound and Vibration* 160 (1993) 372–377.
[10] M. Swaminadham, M. Chinta, Vibration of rotating turbo machine blades with flexible roots, *Journal of Sound and Vibration* 174 (1994) 284–288.
[11] W.J. Haering, R.R. Ryan, R.A. Scott, A new flexible body dynamic formulation for beam structures undergoing large overall motion, *Journal of Guidance, Control and Dynamics* 17 (1994) 76–83.
[12] S.S. Tadikonda, H.T. Chang, On the geometric stiffening in flexible multibody dynamics, *Journal of Sound and Acoustics* 117 (1975) 452–461.
[13] H.H. Yoo, R.R. Ryan, R.A. Scott, Dynamics of flexible beams undergoing large overall motions, *Journal of Sound and Vibration* 181 (1995) 261–278.

[14] H. El-Absy, A.A. Shabana, Geometric stiffness and stability of rigid body modes, *Journal of Sound and Vibration* 207 (1997) 465–496.
[15] B.O. Al-Bedoor, M.N. Hamdan, Geometrically nonlinear dynamic model of a rotating beam, *Journal of Sound and Vibration* 240 (2001) 59–72.
[16] M.N. Hamdan, B.O. Al-Bedoor, Nonlinear free vibration frequencies of a rotating flexible arm, *Journal of Sound and Vibration* 242 (2001) 839–853.
[17] B.O. Al-Bedoor, A. Al-Sinawi, M.N. Hamdan, Non-linear dynamic model of an inextensible rotating flexible arm supported on a flexible base, *Journal of Sound and Vibration* 251 (2002) 767–781.
[18] A. El-Sinawi, M.N. Hamdan, Optimal vibration estimation of a non-linear flexible beam mounted on a rotating compliant hub, *Journal of Sound and Vibration* 259 (2003) 857–872.
[19] L.L. Zavodney, A.A. Nayfeh, The nonlinear response of a slender beam carrying a lumped mass to a parametric excitation, *International Journal of Non-linear Mechanics* 24 (1989) 105–125.